JOURNAL OF CATALYSIS 29, 129–137 (1973)

# Molecular Orbital Description of Catalysis by Metal Clusters

ROGER C. BAETZOLD

*Research Laboratories, Eastman Kodak Company, Rochester, New York 14650*

Received September 8, 1972

Extended Hückel and complete neglect of differential overlap (CNDO) molecular orbital calculations were performed for clusters of metallic atoms to determine possible catalytic properties. Data for pure clusters of Ag, Pd, Cd, Cu, and Ni are reported, as well as for alloy systems of Pd–Ni and Cu–Ni. The results indicate the presence of *d*-band holes in Ni and Pd clusters with a greater amount in Ni. Clusters of Ag and Cd have as low energy form the linear geometry in preference to other three-dimensional geometries. Clusters have a low bond energy (BE) and a different electronic configuration than their bulk metals. The effect of substrates on metal clusters is examined and is shown to be capable of altering electron occupancy of the cluster.

## Introduction

This investigation involves the use of calculation methods to describe the electronic properties of small metal and semiconductor clusters (*1*, *2*). The size range of these clusters is limited to below about 30 atoms, so the particles have very high surface/volume ratios. These size particles play an important role in several catalytic phenomena (*3*). The photographic process relies heavily on catalysis in the chemical reduction of silver halide by small silver clusters produced photochemically and thought to contain four or more atoms (*4*). Other reactions, such as hydrogenation of cyclopropane (*5a*) or ethylene (*5b*), show no dependence of catalytic activity on particle size. The work of Hamilton and Logel (*6*) has demonstrated that metal clusters supported on carbon show a dependence of catalytic activity on size for the deposition of metal ions from solution by reducing agent. An explanation on a molecular scale of why this size-dependent catalytic activity is present for only some reactions is unknown at present. The calculations described below determine electronic properties of metal clusters which are correlated with their catalytic properties.

The effect of substrate on catalyst activity is currently under investigation (*6*). Some reactions reflect this interaction, while others do not (*7*). Calculations described below are designed to examine this possible effect. The effects of mixing two dissimilar metals may also be investigated by this technique, as has been done for the Cu–Ni and Pd–Ni alloy system. A great number of experimental data exist for catalysis in the Cu–Ni system (*8*).

The semiempirical molecular orbital methods used in this work are extended Hückel (EH) (*9*) and complete neglect of differential overlap (CNDO) (*10*). These techniques are relied upon to predict trends in sets of data and qualitative factors which may be responsible for catalysis. Details of the computation have been set forth in earlier work (*1*, *2*), so only the general features will be repeated.

The molecular orbital procedures are used to calculate an energy of the system by variation of coefficients in the wavefunction. The wavefunction of the system is composed of a linear combination of atomic orbitals

$$\psi_i = \sum_j C_{ji}\chi_j, \tag{1}$$

where $\psi_i$ $i$th molecular orbital
$C_{ji}$ coefficient of atomic orbital
$\chi_j$ Slater atomic orbital.

The Slater atomic orbitals, determined by Hartree-Fock atomic calculation (*11*), are available for all elements and have the form

$$\chi_j = Ar^{n-1}e^{-\alpha r}y_{l,m}(\theta,\varphi), \tag{2}$$

$A$ normalizing constant
$n$ principal quantum number
$r$ distance from atom
$\alpha$ exponent determined by Hartree-Fock atomic calculation
$y_{l,m}(\theta,\varphi)$ spherical harmonic.

Variation of the $C_{ji}$ to achieve an energy minimum gives a secular matrix equation of the form

$$|H - ES| = 0, \tag{3}$$

where $H$ = Hamiltonian matrix, $S$ = overlap matrix and $E$ = energy matrix. In the EH method, the diagonal $H_{ii}$ elements are given by

$$-H_{ii} = \text{VSIP (valence state ionization potential for orbital } i) \tag{4}$$

where the ionization potential data are given by atomic ionization potentials or are available by use of spectroscopic data (*12*). The off diagonal elements are calculated by the Wolfsberg-Helmholz formula

$$H_{ij} = \tfrac{1}{2}KS_{ij}(H_{ii} + H_{jj}), \tag{5}$$

where $K$ = constant and

$$S_{ij} = \int \chi_i\chi_j d_\tau. \tag{6}$$

The $E$ matrix is found by diagonalization of Eq. (3) and contains the energy levels ($\epsilon_i$) of the system. Thus, the energy of the system is calculated by

$$E = \sum_i \epsilon_i n_i \tag{7}$$

where $n_i$ = number of electrons in $i$th molecular orbital.

The CNDO procedure involves solution of Eq. (3), but the $S$ matrix is replaced by the unit matrix. The elements of the $H$ matrix are calculated by explicitly taking into account electron–electron repulsion. This leads to a complicated set of formulas previously described (*1*, *2*). Diagonalization of the secular equation provides the energy levels and wavefunctions of system. Parameters used in these calculations are listed in Table 1.

TABLE 1
PARAMETERS USED IN CALCULATION

| Atom | $K$ | Orbital | IP (eV) | Slater exponent ($\alpha$) |
|---|---|---|---|---|
| | | EH | | |
| Ag | 1.30 | 5*p* | 3.83 | 1.35 |
| | | 5*s* | 7.56 | 1.35 |
| | | 4*d* | 11.58 | 3.61 |
| Cd | 1.90 | 5*p* | 4.19 | 1.64 |
| | | 5*s* | 8.96 | 1.64 |
| | | 4*d* | 17.66 | 3.97 |
| Pd | 1.44 | 5*p* | 2.00 | 1.57 |
| | | 5*s* | 7.32 | 1.57 |
| | | 4*d* | 8.33 | 3.40 |
| | | CNDO | | |
| | $\beta^0$ | | $\frac{1}{2}$ (IP + EA) | |
| Ni | −7 | 4*p* | 1.92 | 1.43 |
| | | 4*s* | 4.70 | 1.43 |
| | | 3*d* | 4.97 | 4.18 |
| Cu | −1 | 4*p* | 2.56 | 1.46 |
| | | 4*s* | 4.45 | 1.46 |
| | | 3*d* | 5.96 | 4.40 |

## RESULTS

### *Metal Clusters*

In general the properties of small clusters of atoms are intermediate between bulk and single-atom values. For example, the average bond energy per atom (BE/atom) is plotted versus number of atoms for silver clusters in Fig. 1. Here, there is an increase in BE/atom, which may approach for bulk the cohesive energy (2.96 eV) of Ag. The difference in cohesive energy (CE) and BE/atom gives the surface energy (SE) according to:

$$\text{SE} = \text{CE} - \text{BE/atom}. \tag{8}$$

Surface energy is almost double the BE/atom for Ag particles in Fig. 1. In addition,

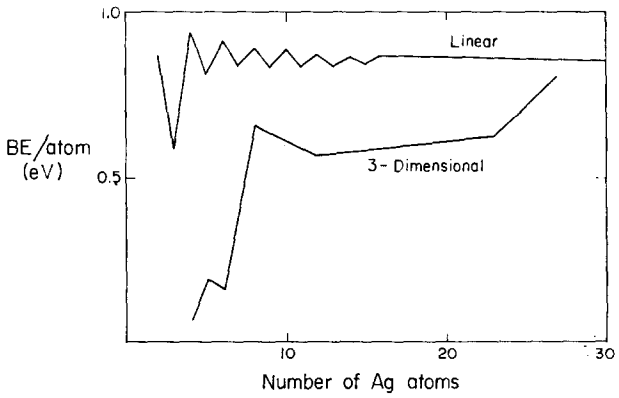


FIG. 1. Average BE/atom for Ag particles versus number of atoms.

a linear array is shown to be the more stable form of small clusters. Continuation of the trends indicated in Fig. 1 would result in the three-dimensional aggregate becoming the stable form of Ag at about 50 atoms.

The work function for a bulk metal is equal to the ionization potential (IP) of the metal and is equal to the electron affinity (EA) of the metal. Here, IP is the energy required to take an electron from the cluster to vacuum and EA is the energy released on placing an electron from vacuum on the cluster. In small clusters, IP > EA, as shown for Ag in Fig. 2. These data predict a semiconductor nature of the cluster. Here IP is identified with the highest occupied molecular orbital (HOMO) and EA is identified with the lowest unoccupied molecular orbital (LUMO). The trends in these quantities with size are significant. As size increases, IP decreases from the value 7.56 eV for atomic Ag towards the work function 4.5 eV. The IP approaches 7.0 eV for linear aggregates (Fig. 2) and it approaches 5.5 eV for three-dimensional aggregates (*1*). The EA increases with size of Ag cluster, converging on the work function. This trend in EA is important since electron transfer to the metal cluster requires a high EA.

The odd–even behavior of Ag particles, shown in Fig. 2, results from a doubly occupied or singly occupied HOMO. Particles with even numbers of electrons have higher BE/atom and IP, but lower EA than similar-sized particles with an odd number of electrons.

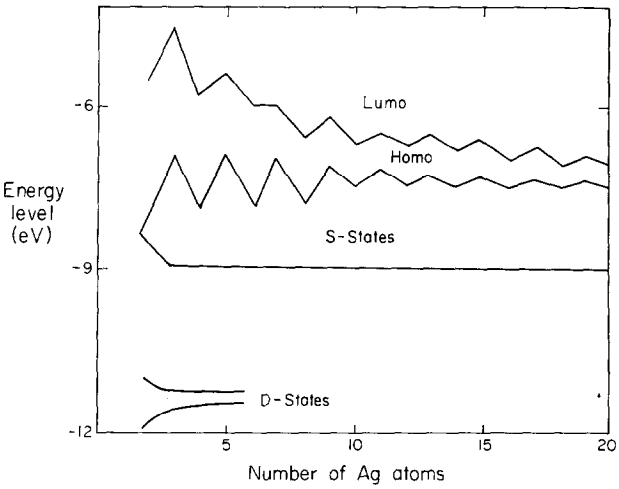


FIG. 2. Band structure of linear Ag aggregates versus number of atoms.

Extended Hückel calculations show an expansion of lattice constant with size from 2.10 Å for $Ag_2$ to 2.65 Å for $Ag_{10}$, at which point it remains nearly constant for the linear particles. This effect, as well as the decrease in IP with size, is caused by occupancy of antibonding molecular orbitals which are less stable than their corresponding atomic orbitals and are of a repulsive nature.

Calculations for Pd (atomic configuration $4d^{10}$) indicate that it behaves similarly to Ag with regard to trends in BE/atom, IP and EA. Three-dimensional symmetric geometries are more stable than linear geometries for the small Pd particles. An interesting feature of Pd clusters is that LUMO is composed of *d* orbitals and not *s* orbitals as the atomic level ordering would suggest. This presence of *d*-holes occurs in small size clusters like $Pd_2$ because the diffuse *s* atomic orbitals overlap strongly and form a low-energy symmetric molecular orbital. Electrons occupy this molecular orbital leaving a vacant *d* molecular orbital. As the size of the Pd cluster increases, the number of unoccupied *d* molecular orbitals increases.

Cadmium clusters (atomic configuration $4d^{10}5s^2$) are weakly stable, as shown by the data derived from EH calculation in Table 2. Linear geometry is more stable than symmetric three-dimensional geometries or even the bulk crystal structure for the small Cd clusters. Poor stability is a consequence of the closed atomic 5*s* shell in Cd. Unstable antisymmetric 5*s* molecular orbitals are filled in the small clusters, but the amount of bonding by 5*p* orbitals increases with size. This leads to the trend of increasing stability with size as observed in Table 2. Comparison of the calculated data with experimental data shows that the calculations correctly predict the trends in BE/atom, IP and EA as size increases.

Nickel clusters behave similarly to Pd clusters. The Ni atomic configuration ($3d^84s^2$) indicates that LUMO is expected to be of *d* character. Symmetric three-dimensional geometries are the most stable geometry and data in Table 3 indicate trends in BE/atom, IP and EA similar to those described before (*1*) for Pd and other metal clusters. The set of *d* orbitals of Ni clusters have smaller fractional occupancy than the set of *d* orbitals of Pd clusters, although LUMO in both cases has *d* character.

Calculations by CNDO support the general conclusions of EH for the Ni clusters.

TABLE 2
EXTENDED HÜCKEL CALCULATIONS FOR Cd CLUSTERS[a]

| Cluster | Geometry | BE/atom (eV) | Req (Å) | IP (eV) | EA (eV) |
|---|---|---|---|---|---|
| 2 | Linear | 0.29 | 2.0 | 6.30 | 5.38 |
| 3 | Linear | 0.43 | 2.0 | 5.72 | 5.72 |
| 3 | Triangle | 0.40 | 2.25 | 7.18 | 5.81 |
| 4 | Linear | 0.64 | 2.25 | 5.68 | 5.68 |
| 4 | Pyramid | 0.41 | 2.50 | 5.62 | 5.42 |
| 5 | Linear | 0.74 | 2.25 | 5.75 | 5.75 |
| 5 | Bipyramid | 0.02 | 2.75 | 5.52 | 5.30 |
| 15 | Linear | 0.96 | 2.50 | 5.68 | 5.68 |
| 15 | Hexagonal-close-pack | 0.19 | 2.50 | 6.11 | 5.71 |
| 28 | Hexagonal-close-pack | 0.23 | 2.75 | 5.82 | 5.77 |
| | | Experimental data | | | |
| 2 | Linear | 0.09[b] | 2.46[c] | — | — |
| Bulk | Hexagonal-close-pack | 1.16 | 2.97 | 4.1 | 4.1 |

[a] $K = 1.90$.
[b] Drowart, J., and Honig, R. E., *J. Phys. Chem.* **61**, 980 (1957).
[c] Sum of covalent radii.

TABLE 3
Ni AGGREGATES—EXTENDED HÜCKEL CALCULATION[a]

| No. of atoms | Geometry | BE/atom (eV) | HOMO (eV) | LUMO (eV) | *d*-Holes/atom |
|---|---|---|---|---|---|
| 2 | Linear | 1.31 | 7.63 | 7.63 | 1.0 |
| 3 | Equilateral triangle | 1.34 | 7.63 | 7.63 | 0.67 |
| 4 | Pyramid | 1.24 | 7.63 | 7.63 | 0.50 |
| 5 | Bipyramid | 1.11 | 7.63 | 7.63 | 0.40 |
| 6 | Square bipyramid | 1.03 | 7.63 | 7.63 | 0.36 |
| 8 | Cube | 1.01 | 7.63 | 7.63 | 0.70 |
| | | Experimental data | | | |
| | | BE/atom (eV) | IP (eV) | Req (Å) | |
| 2 | Linear | 1.2[b] | 6.4[c] | 2.30[b] | |
| Bulk | fcc | 4.44 | 4.5–5.2 | 2.49 | |

[a] Req = 2.5 Å.
[b] Kant, A., *J. Chem. Phys.* **41,** 1872 (1964).
[c] Schissel, P., *J. Chem. Phys.* **26,** 1276 (1957).

One weakness of the EH calculation is the lack of dependence of position of energy level on occupancy, which results in the constant behavior of HOMO and LUMO in Table 3. The CNDO method produces energy levels sensitive to occupancy and calculation yields HOMO = 7.61 eV for $Ni_2$ and HOMO = 6.20 eV for $Ni_6$. The opposite trend is observed for LUMO, which equals 2.32 eV for $Ni_2$ and 4.43 eV for $Ni_6$. The convergence of HOMO and LUMO with increasing size was observed for other elements.

The electronic occupancy of the valence orbitals for large clusters of each element is shown in Table 4. This occupancy is determined by analysis of the atomic orbitals which are occupied in each molecular orbital. The Engel-Brewer procedure (*13*) leads to predictions of electronic configuration based upon crystal structure. The number of bonding *s* and *p* electrons progresses from one to two to three as the bulk crystal structure changes from body-center-cubic, hexagonal-close-pack to cubic-close-pack, respectively. Our calculations indicate a higher degree of occupancy of the *d* orbitals and a lower degree of occupancy of the *p* orbitals than the Engel-Brewer procedure. A source of the disagreement may be the finite size clusters employed for the calculation since there are indications from the calculated stable geometric forms of each metal that the bonding is different in cluster and bulk.

The prediction of linear geometry for small metal clusters of Ag and Cd is not unreasonable in light of recent experiments with the field ion microscope (*14–16*). The calculations apply to isolated

TABLE 4
ELECTRONIC CONFIGURATION OF CLUSTERS

| Cluster | Geometry | Calculation | Configuration | Engel-Brewer configuration |
|---|---|---|---|---|
| $Ni_7$ | Square bipyramid | CNDO | $d^{8.85}s^{.49}p^{.66}$ | $d^7s^1p^2$ |
| $Cd_{15}$ | Hexagonal-close-pack | EH | $d^{10}s^{1.45}p^{.55}$ | $d^{10}s^1p^1$ |
| $Cu_8$ | Cube | CNDO | $d^{10}s^{.86}p^{.14}$ | $d^8s^1p^2$ |
| $Ag_8$ | Cube | CNDO | $d^{10}s^{.70}p^{.30}$ | $d^8s^1p^2$ |
| $Pd_8$ | Cube | CNDO | $d^{9.45}s^{.29}p^{.26}$ | $d^7s^1p^2$ |

clusters not interacting with a substrate, while the experiments involve atom clusters on a surface such as tungsten. Tsong (*14, 15*) has observed chains of up to six W atoms on the W(211) surface and Bassett (*16*) has observed linear clusters of both Pt and Ir on the W(110) surface. Other work has shown that the cluster geometry takes various nonlinear forms for W and Re atoms on the W(110) surface. These experiments illustrate the complex nature of the interaction between cluster atoms and substrate that controls the cluster geometry. They suggest, as these calculations illustrate, that there is a significant difference in bonding in small clusters and bulk metals.

*Alloy Models*

Models containing Ni and Pd, which represent alloys, have been examined by EH-type calculation. Table 5 shows the properties of $Pd_2$ with various amounts of Ni. The properties of NiPd particles are very close to the properties of Ni particles, as shown by comparing data in Tables 3 and 5. The *d*-band holes are removed from Pd by electron transfer from Ni and LUMO is composed of Ni *d* atomic orbitals in the alloy. These effects are caused because the *s* and *d* valence atomic orbitals in Ni are higher in energy than the corresponding *s* and *d* atomic orbitals in Pd. This general effect in alloying causes the wavefunction of HOMO and LUMO and the IP and EA of alloys to have properties more like those of the atom with smallest IP. Experimental measurements (*17*) of the relative magnetic moment in these alloys show a decreasing moment as Pd fraction increases. This magnetization is due to holes in the Ni *d*-band since there are negligible holes in the Pd *d*-band, as shown in Table 3.

TABLE 5
EH CALCULATION FOR $Pd_2Ni_N$ AGGREGATES

| *N* | BE/atom (eV) | EA (eV) | Character of LUMO | Total Pd *d*-holes |
|---|---|---|---|---|
| 0 | 0.40 | 8.16 | Pd *d* orbitals | 2.0 |
| 1 | 1.17 | 7.63 | Ni *d* orbitals | 0.04 |
| 2 | 1.16 | 7.63 | Ni *d* orbitals | 0.10 |
| 3 | 1.09 | 7.63 | Ni *d* orbitals | 0.25 |
| 4 | 1.01 | 7.55 | Ni *d* orbitals | 0.26 |

We have examined square four-atom Cu–Ni clusters of varying composition since these clusters may serve as a model for the Cu–Ni alloy. The catalytic properties of this alloy for such reactions as hydrogenation are well known (*8*). It is generally found that adding Cu to Ni diminishes catalytic activity. This effect is generally attributed to filling of *d*-band holes in Ni by Cu, which is complete at 60% Cu. Figure 3 shows the nature of HOMO and LUMO in these alloys and is in accord with the above interpretation. The identification of the major component of the wavefunction shows that in the con-

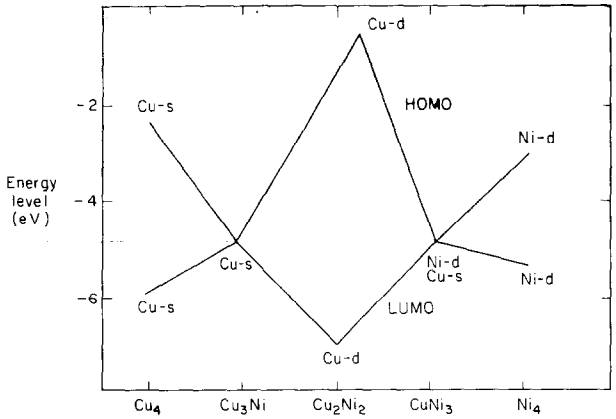


FIG. 3. Character of HOMO and LUMO in Cu–Ni alloys consisting of four atoms in a square of side length 3 Å.

centration range 50–75% Cu, *d* orbitals are no longer present in HOMO or LUMO. The symmetry properties of *d* orbitals facilitate $H_2$ adsorption and dissociation and will be discussed later. The total binding energy of $Cu_nNi_{4-n}$ aggregates has a maximum for $n = 2$ and is almost twice as large as the binding energy of $Cu_4$ or $Ni_4$. This suggests that mixing of the two components would occur whenever possible, and in this state, catalysis involving *d*-holes is impeded.

These calculations for Cu–Ni alloys may be compared with recent Auger results (*18*, *19*) and X-ray appearance spectra data (*20*). In a series of alloys prepared by melting varying ratios of Cu and Ni, the surface composition was shown to be the same as the bulk composition. Appearance potential spectra were used to show the states that are occupied in surface atoms. It was found that Cu addition causes a decrease in the number of Ni *d*-holes, but that at even greater than 55% Cu, *d*-holes are still present on Ni. The trend of decreasing Ni *d*-holes with Cu addition is observed in the calculation as Fig. 3 illustrates. The calculations do not show the presence of Ni *d*-holes at greater than 55% Cu in contrast to the experiments. Larger cluster models would be helpful to resolve this effect.

### *Catalytic Factors*

Some factors responsible for catalysis by metal clusters have been indicated. Larger clusters are better catalytic centers than small clusters because of the trends in BE/atom and EA with size. Larger clusters can bind atoms more strongly than small clusters. This might be important in reactions involving reduction of ions and deposition in a solid phase. The effect of size on EA is to make larger particles better electron acceptors; a role they may play in some catalytic process. Thus, these two effects argue for an increase in catalytic activity with size.

An important factor in catalysis is the symmetry of HOMO and LUMO. Recent discussions (*21*, *22*) have indicated the role that orbital symmetry plays in homogeneous reactions and many of the same considerations apply to heterogeneous reactions. The HOMO and LUMO of Pd and Ni clusters is composed of an antisymmetric combination of *d* orbitals. The directional character of *d* orbitals makes them particularly suitable for positive overlap with reactant molecules. The symmetry of these orbitals, however, allows reactions to occur which, in their absence, would have a very high activation energy. A simple example is the addition of $H_2$ to $O_2$, which is symmetry forbidden because of the nonmatching of orbital parity shown in Fig. 4. In the presence of transition metal, $H_2$ is adsorbed and dissociates to atoms which do not have symmetry restrictions for reaction with $O_2$.

### *Substrate Effect*

The effect of carbon substrate on Pd clusters has been examined by extended Hückel calculation. The carbon model consisted of 10 C atoms in the form of two adjacent hexagons. When Pd atoms are placed in contact with carbon, there is destabilization of the Pd molecular orbitals. The 5*s* orbitals of Pd are more diffuse than 4*d* orbitals and are destabilized more, so that LUMO no longer has *d* character. This is observed for clusters containing up to six Pd atoms in contact with the carbon surface. When some of the Pd atoms are placed

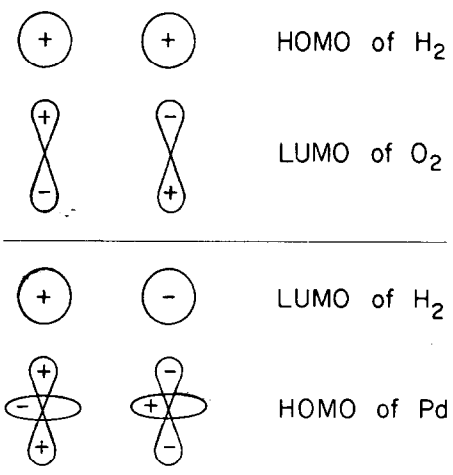


FIG. 4. Example of a symmetry forbidden reaction ($H_2 + O_2$) and a symmetry allowed reaction ($H_2 + Pd$).

above other Pd atoms and not in direct contact with the lattice, LUMO acquires *d* character. This indicates that the first monolayer of metal has quite different properties than pure Pd owing to interaction with the substrate.

The destabilization of adsorbed-atom energy levels has been examined by comparing $Pd_2$ on substrates represented by a plane of nine atoms of pure B, Li, Cu, or Al, all having bulk nearest-neighbor distances. It is found that the condition necessary for LUMO to have *d* character is to have 5*s* orbitals of Pd to lie below occupied energy levels of atoms in the substrate. Thus, in the cases of Al, Li, and Cu, LUMO has *d* character, but in the case of B and C it has no *d* character. In the latter cases, the IP of B and C is greater than the IP of the 5*s* level of Pd (7.33 eV).

Calculations by CNDO for Pd on the carbon model are more quantitative than calculations by EH. These indicate that a single Pd atom is bound by 3.24 eV at 2.0 Å over a C atom. Addition of another Pd atom to the carbon produced a small increase in bonding energy, but does not result in twice the bond energy of a single atom. This suggests Pd atoms would not aggregate on planar carbon. A special site or impurity would be a location necessary for aggregation. Other metals, such as Ag, Cu, Ni, and Zn, are calculated to be similar in behavior. Apparently the carbon model is very reactive towards a single atom, but valence becomes saturated with one atom and reactivity to further atoms is diminished. Perhaps part of a monolayer of atoms is used to saturate a carbon surface and become bound very tightly. Upon satisfying this surface valence, Pd atoms bonded to other Pd atoms and not the carbon surface are responsible for catalytic effects measured on carbon surfaces.

Previous molecular orbital calculations have examined the effect of substrate on adsorbing species. Extensive work has been done for the interaction of graphite with atomic H, F, O and N by CNDO calculation (*23*). Consideration of the symmetries of the wavefunctions of the graphite substrate and the chemisorbed atom has led to rules for chemisorption. The basis for these rules is very similar to the considerations (*21*, *22*) that lead to the behavior predicted in Fig. 4.

The adsorption properties of a transition metal surface of Ni have been examined using EH in recent papers (*24*, *25*). Adsorption of hydrogen atoms to Ni surfaces has shown that the bonding involves interaction of $3d_{Z^2}$ and 4*s* orbitals of Ni with 1*s* orbitals of H. These calculations confirm the importance of antisymmetric combinations of *d* orbitals with $e_g$ symmetry in the bonding between Ni and H, such as depicted in Fig. 4. The calculations of adsorbed CO on the Ni surface have shown that the stable configuration has CO perpendicular to the surface and is bonded through C. The binding energy per CO molecule is found to increase when several CO molecules are placed at special positions on the nickel model. The binding energy per Pd unit on the 10-atom carbon model decreases with number of Pd atoms adsorbed. These opposing effects indicate the sensitivity of molecular orbital calculations to geometry and the electronic nature of substrate and adsorbate.

## Conclusions

A. Earlier calculated properties for Ag and Pd clusters have been compared with data for Ni and Cd clusters to determine how nuclei can act as catalysts. The catalysts provide centers for accepting electrons from reducing agents or centers for binding metal atoms that have just been reduced. In addition, symmetry of HOMO and LUMO wavefunctions is important in catalysis. Atoms with *d* orbitals in these wavefunctions have the correct symmetry for hydrogenation catalysis.

B. Alloys of Cu–Ni show properties similar to those deduced by catalytic experiments. Catalysis is possible through the action of *d*-band holes which are calculated to be present in the HOMO of the alloy only when copper is present in less than 50%. Experiments on bulk alloys conflict with this calculation.

C. Catalysis by Pd clusters is sensitive to the substrate. The substrates having

atoms with IP $< 7.33$ eV leave $d$-holes in Pd.

D. Catalysis by Pd clusters can be changed by alloying since $d$-holes are removed from Pd by alloying with Ni. A rough guide as to whether Pd retains $d$-holes on alloying can be suggested. If the new atom has IP $< 7.33$, Pd $d$-holes should be retained. If the new atom has IP $> 7.33$, Pd $d$-holes should be removed.

## References


1. Baetzold, R. C., *J. Chem. Phys.* **55,** 4363 (1971).
2. Baetzold, R. C., *J. Solid State Chem.,* in press.
3. Figueras, F., Mencier, B., DeMourgues, L., Naccache, C., and Trambouze, Y., *J. Catal.* **19,** 315 (1970).
4. Mees, C. E. K., and James, T. H., "The Theory of the Photographic Process," 3rd ed. Macmillan, New York, 1966.
5. (a) Boudart, M., Aldag, A., Benson, J. E., Dougharty, N. A., and Harkins, C. G., *J. Catal.* **6,** 92 (1966). (b) Dorling, T. A., Eastlake, M. J., and Moss, R. L., *J. Catal.* **14,** 23 (1969).
6. Hamilton, J. F., and Logel, P. C., *J. Catal.,* in press.
7. Taylor, W. F., Yates, D. J. C., and Sinfelt, J. H., *J. Phys. Chem.* **68,** 2962 (1964).
8. (a) Sachtler, W. M. H., and Jongepier, R., *J. Catal.* **4,** 665 (1965). (b) Van der Plank, P., and Sachtler, W. M. H., *J. Catal.* **12,** 35 (1968).
9. Hoffmann, R., *J. Chem. Phys.* **39,** 1397 (1963).
10. Pople, J. A., Santry, D. P., and Segal, G. A., *J. Chem. Phys.* **43,** S129 (1965).
11. Clementi, E., and Raimondi, D. L., *J. Chem. Phys.* **38,** 2686 (1963).
12. Moore, C. E., *Nat. Bur. Stand. (U. S.) Circ.,* **467,** Vols. 1-3 (1949).
13. Brewer, L., *Science* **161,** 115 (1968).
14. Tsong, T. T., *Phys. Rev. B.* **6,** 417 (1972).
15. Tsong, T. T., *J. Chem. Phys.* **55,** 4658 (1971).
16. Bassett, D. W., *Surface Sci.* **21,** 181 (1970).
17. Kimura, H., Katsuki, A., and Shimizu, M., *J. Phys. Soc. Jap.* **21,** 307 (1966).
18. Quinto, D. T., Sundaram, V. S., and Robertson, W. D., *Surface Sci.* **28,** 504 (1971).
19. Ertl, G., and Küppers, J., *Surface Sci.* **24,** 104 (1971).
20. Ertl, G., and Wandelt, K., *Phys. Rev. Lett.* **29,** 218 (1972).
21. (a) Pearson, R. G., *Theoret. Chim. Acta* **16,** 107 (1970). (b) Pearson, R. G., *Chem. Eng. News,* Sept. 28, 1970, p. 66.
22. Hoffmann, R., *Accounts Chem. Res.* **4,** 1 (1971).
23. (a) Bennett, A. J., McCarroll, B., and Messmer, R. P., *Surface Sci.* **24,** 191 (1971); (b) Bennett, A. J., McCarroll, B., and Messmer, R. P., *Phys. Rev. B* **3,** 1397 (1971); (c) Messmer, R. P., and Bennett, A. J., *Phys. Rev. B* **6,** 633 (1972).
24. Robertson, J. C., and Wilmsen, C. W., *J. Vac. Sci. Technol.* **9,** 901 (1972).
25. Fassaert, D. J. M., Verbeek, H., and Van der Avoird, A., *Surface Sci.* **29,** 501 (1972).